Electronic Supplementary Information

Laser-Induced Graphitization of Colloidal Nanodiamonds for Excellent Oxygen Reduction Reaction Catalytic Activity

Dong Myung Jang, Hyung Soon Im, Seung Hyuk Back, Kidong Park, Young Rok Lim, Chan Su Jung, Jeunghee Park, and Minyung Lee

Figure S1. (a) ORR CV curve of Pt/VC in O_2-saturated 0.1 M KOH solution, along with O_2-free current. LSV curves at rotation speed of 400~2500 rpm and K-L plot at potentials varying from -0.3 to -0.8 V for (b), (c) Pt/VC and (d), (e) GND. The *n* values for GND were increased from 2.4 to 3.8 (avg. 3.0) as the applied voltage increased, indicating they are mainly two electron transfer at low voltage and four electron at high voltage in oxygen reduction process. The *n* value for Pt/VC was 4.0 for all applied voltages.

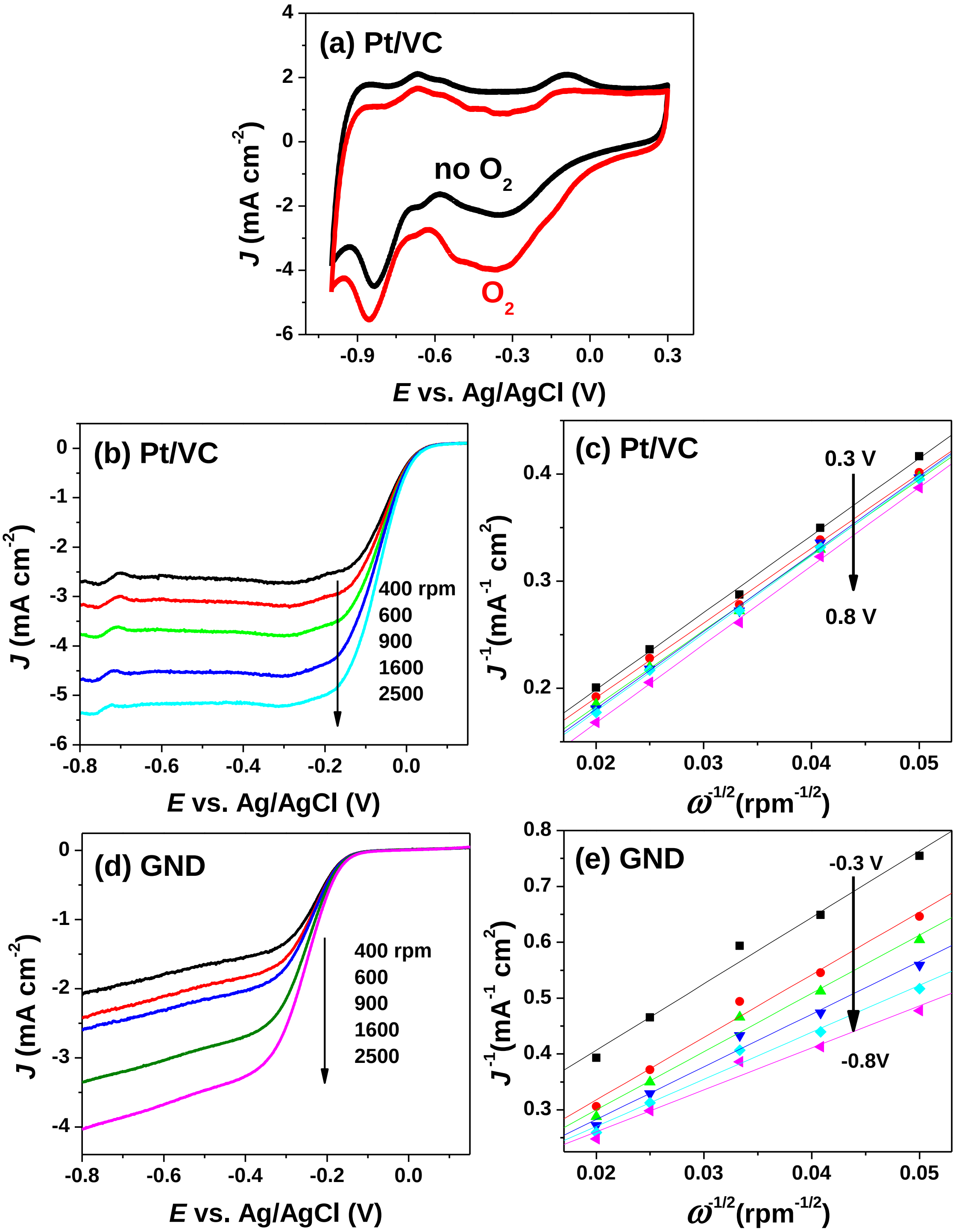
(a) Pt/VC
no O2
O2
J (mA cm-2)
4
2
0
-2
-4
-6
-0.9
-0.6
-0.3
0.0
0.3
E vs. Ag/AgCl (V)
(b) Pt/VC
400 rpm
600
900
1600
2500
J (mA cm-2)
0
-1
-2
-3
-4
-5
-6
-0.8
-0.6
-0.4
-0.2
0.0
E vs. Ag/AgCl (V)
(c) Pt/VC
0.3 V
0.8 V
J-1(mA-1 cm2)
0.4
0.3
0.2
0.02
0.03
0.04
0.05
ω-1/2(rpm-1/2)
(d) GND
400 rpm
600
900
1600
2500
J (mA cm-2)
0
-1
-2
-3
-4
-0.8
-0.6
-0.4
-0.2
0.0
E vs. Ag/AgCl (V)
(e) GND
-0.3 V
-0.8V
J-1(mA-1 cm2)
0.8
0.7
0.6
0.5
0.4
0.3
0.02
0.03
0.04
0.05
ω-1/2(rpm-1/2)

Figure S2. CV curves of (a) N-GND and (b) Pt/VC electrode in O_2-saturated 0.1 M KOH/3.0 M MeOH solution, and (c, d) cathodic ORR current vs. time at applied voltage of -0.2 V. Arrow indicates the addition of 3.0 M MeOH into O_2-saturated electrochemical cell. For the N-GND, there is no change in O_2 reduction current upon the addition of MeOH, showing electrocatalytic selectivity for O_2 that evades the crossover effect of alcohol. However, the the ORR peak at about -0.15 V vanished in the CV curves of the Pt/VC electrode when the 3M MeOH is added in the O_2-saturated 0.1 M KOH solution. Furthermore, the cathodic ORR current shifted from a cathodic current to a reverse anodic current after the addition of MeOH. It indicates that N-GND holds high promise for use as cathode in methanol and alkaline fuel cells.

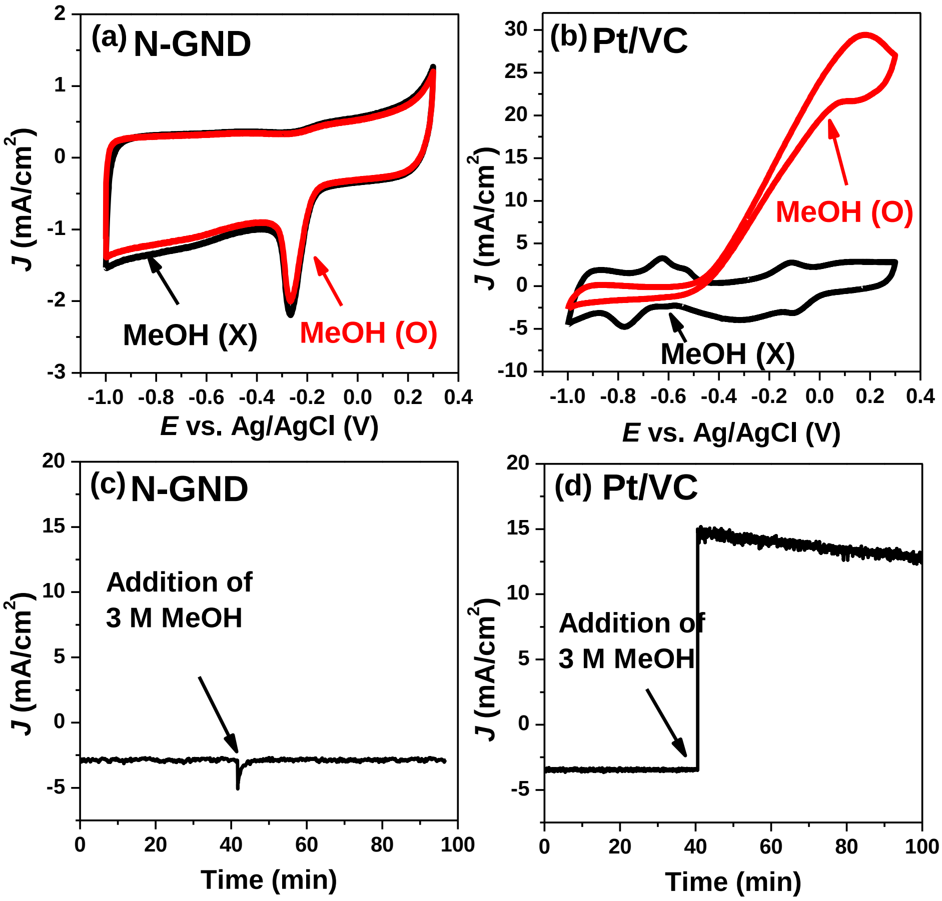

Figure S3. N_2 adsorption-desorption isotherms (at 77 K) of (a) ND (pristine), (b) HND (after H_2 treatment of acid-purified ND at 800 ˚C), (c) GND (graphitized ND after 10 min laser irradiation using ethanol solution and H_2 treatment), (d) GND (graphitized ND after 30 min laser irradiation using ethanol solution and H_2 treatment). These isotherm curves were measured on a surface area and pore size measurement apparatus. Before the measurements, the sample was degassed at 300 ºC for 6 h. The specific surface area was calculated via the Brunauer-Emmett-Teller (BET) model at relative pressures of P/P_0 = 0.20. The total pore volume was estimated from the uptake of adsorbate at a relative pressure of P/P_0 = 0.99. Pore size distributions were derived from the adsorption branches of the isotherms using the Barrett–Joy–Halenda (BJH) model. The results are summarized in Table S1.

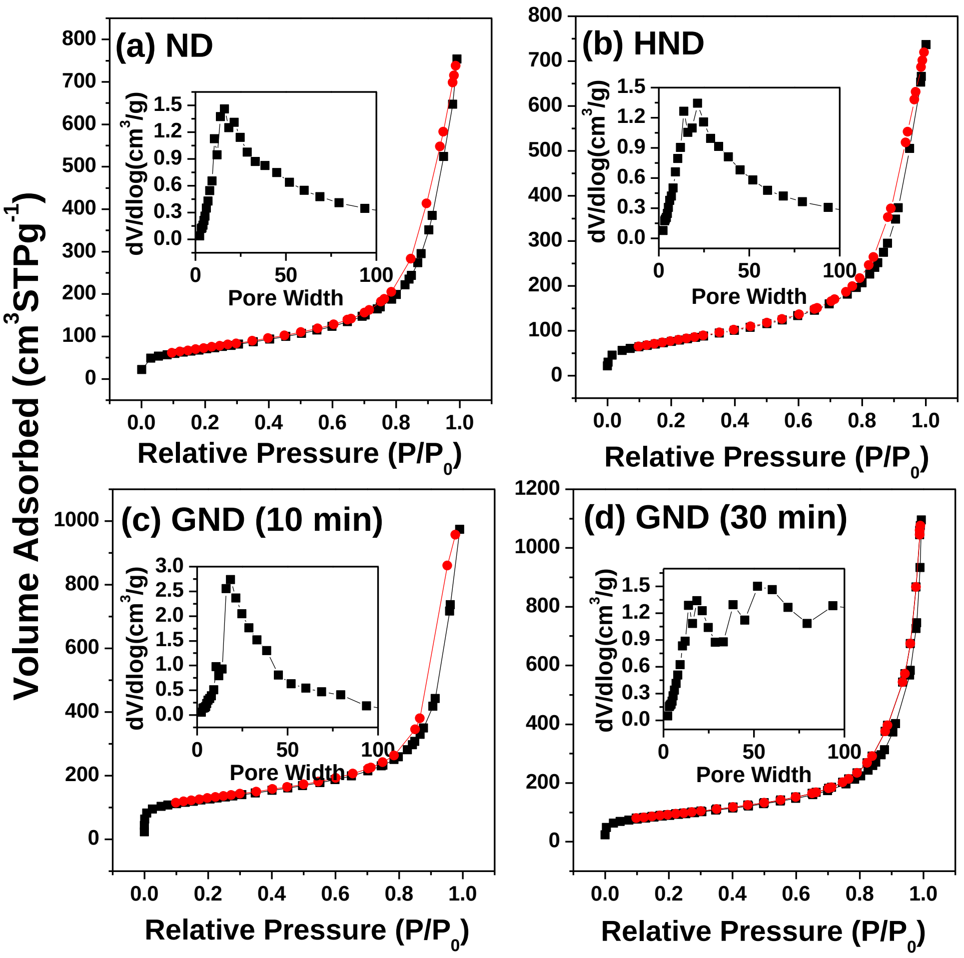

Table S1. Pore structure parameters of samples derived from the N_2 adsorption-desorption isotherms

Sample	S_{BET}(m^2/g)[a]	V_{BJH}(cm^3/g)[b]	D_{BJH}(nm)[c]
ND (pristine)	253.1	1.15	18.1
HND	274.2	1.06	15.5
GND (10 min)	426.4	1.50	14.0
GND (30 min)	312.2	1.50	19.2

[a] BET specific surface area; [b]BJH pore volume; [c]BJH average pore diameter.

The BET surface area of ND and HND is 253.1 and 274.2 m^2/g, respectively. The increase of BET surface areas, Barrett–Joy–Halenda (BJH) pore volume, and BJH average pore size in the GND sample can be attributed to the graphitization. These values are consistent with those of graphitized NDs that were synthesized using high-temperature annealing process (>1600 °C). As the irradiation time increases to 30 min, the surface area decreases, probably due to the aggregation into a cage-like structure.